Polycyclic Aromatic Hydrocarbons from Particulate Matter 2.5 (PM2.5) in Polluted Air Changes miRNA Profile Related to Cardiovascular Disease

Authors' Contribution:
Study Design A
Data Collection B
Statistical Analysis C
Data Interpretation D
Manuscript Preparation E
Literature Search F
Funds Collection G

AE 1 **Xiaonan He**
DE 2 **Yu Chen**
F 2 **Cheng Zhang**
BC 1 **Wei Gong**
BC 1 **Xinyong Zhang**
G 1 **Shaoping Nie**

1 Emergency Citical Care Center, Beijing AnZhen Hospital, Capital Medical University, Beijing, P.R China
2 Department of Cardiology, China-Japan United Hospital Affiliated Jilin University, Changchun, Jilin, P.R China

Corresponding Author: Shaoping Nie, e-mail: spnie@126.com
Source of support: The work was supported by the Beijing Municipal Science and Technology Chinese Medicine Development Funds Youth Research Project (grant number QN2016-20) and the Basic/Clinical Scientific Research Cooperation Fund of Capital Medical University (grant number 17JL72). This study was also supported by National Science Foundation Council of China (No. 81700383), Jilin provincial industrial innovation special fund project (No. 2016C041)

Background: Particulate matter 2.5 (PM2.5) in air pollution is regarded as a risk factor for cardiovascular disease (CVDs). Recently, it has become well accepted that polycyclic aromatic hydrocarbons (PAHs) in PM2.5 impacts human CVDs. However, few studies have shown miRNAs affected by PAHs play a critical role in transcriptional regulation related to cardiovascular development and disease.

Material/Methods: Human umbilical cord vein cells (HUVECs) incubated prior to treatment with PAHs at various concentrations (0, 100, 200, 300, 400, and 500 µg/ml) of PAHs particle solutions were added to the culture medium for 24 h. We performed isolation and sequencing of small RNAs and analysis of small RNA sequences and differential expression. The M3RNA database was used to predict miRNA-miRNA interactions. Tools from the DAVID database were used to perform the GO functional analysis of predicted miRNA target genes. A First-Strand cDNA Synthesis Kit was used to synthesis cDNA.

Results: miRNA155 was revealed as a key regulator in PAHs treatment. The putative targets of upregulated miRNA in PAHs treatment indicated that the downregulated genes were enriched in biological pathways such as Wnt signaling and ErbB signaling, which are crucial for the development of vasculature.

Conclusions: In general, our results suggest that PAHs taken by PM2.5 can decrease cardiovascular-related gene expression through upregulating miRNA, which may be a new target for therapy in the future.

MeSH Keywords: **Cardiovascular Diseases • MicroRNAs • Particulate Matter • Polycyclic Hydrocarbons, Aromatic**

Full-text PDF: https://www.medscimonit.com/abstract/index/idArt/908106

📄 3010   ▦ 6   📊 4   📖 31

Background

Particulate matter (PM) with a diameter of less than 2.5 µm (PM2.5) has been identified as the most harmful type of PM. Epidemiological and experimental studies suggest that exposure to air pollution containing PM2.5 increases the risk for cardiopulmonary diseases, cerebrovascular disease, and diabetes [1-3]. Since 2004, the American Heart Association (AHA) has asserted that PM air pollution plays a role in cardiovascular morbidity and mortality [4]. In the last decade, more evidence has accumulated to support PM2.5 exposure as a risk factor of CVDs [5–10]. Polycyclic aromatic hydrocarbons (PAH) are the major pollution in PM2.5 and are composed of multiple aromatic rings. It has been widely accepted that the inflammatory response and oxidative stress may be responsible for PAHs-induced cardiopulmonary diseases. PAHs can induce reactive oxygen species (ROS) production and decrease antioxidant enzyme activity, resulting in oxidative stress in vascular endothelial cells [11].

A disease pathway was established by molecular biology techniques and comprehensive analysis of disease-gene interactions. These interactions are based on the functions of coding genes in disease, including miRNA regulation and protein modification. Recent genomic studies have identified a class of endogenous non-coding RNA molecules with pivotal roles in vascular remodeling and disease [12]. miRNA is a type of small non-coding RNA molecule that is able to downregulate the expression of diverse target genes [13]. Recent studies have identified a group of miRNAs associated with CVDs that are widely distributed in the human genome, including miRNA-126, miRNA-155, and the miRNA gene clusters 143/145, 23/24/27, 17–92, and 14q32 [12,14,15]. However, whether these miRNAs are affected by cardiovascular-localized PAH exposure is unclear. In addition, many other miRNAs affected by PAH exposure remain unclear.

In this study, we profiled miRNA expression in endothelial cells after PAHs taken by PM2.5. Through comparison with the miRNA profile in normal conditions, differentially expressed miRNAs were identified, including many associated with CVDs. A typical bioinformatics algorithm was applied to predict the potential target genes of these miRNAs. The identification of PAHs-regulated miRNAs will facilitate the development of biomarkers for PAHs-induced CVDs and provide new knowledge about the mechanisms by which PAHs affect human health.

Material and Methods

Cell growth and PAHs treatment

Human umbilical cord vein cells (HUVECs) obtained from the American Type Culture Collection (ATCC, Manassas, VA) were cultured in Medium 199 (Life Technologies, Gaithersburg, MD) containing 4 mM L-glutamine, 90 mg/ml heparin, 1 mM sodium pyruvate, 30 mg/ml endothelial cell growth stimulant (Life Technologies), and 20% FBS (HyClone, Logan, UT) at 37°C in an atmosphere of 5% CO_2. Only cells at passages 2 to 4 were used in our experiments. In all experiments, HUVECs were washed and incubated for 24 h prior to treatment with PAHs Different concentrations (0, 100, 200, 300, 400, and 500 µg/ml) of PAHs particle solutions were added to the culture medium for 24 h before MTT assays. The MTT assay was used to determine the IC50 of PAHs and was performed using an MTT assay kit (EMD Millipore) following the manufacturer's protocol. The IC50 of PAHs was calculated by a modified Kou-type method.

Isolation and sequencing of small RNAs

According to the manufacturer's protocol, a miRNeasy mini kit was used for the extraction of total RNA and non-coding RNA (ncRNA) from frozen samples. RNA quality was evaluated by using an Agilent 2100 Bioanalyzer. Small RNA libraries were created from total RNA by using an Illumina TruSeq Small RNA Library Preparation Kit. Total RNA was quantified with a spectrophotometer (NanoDrop 2000) and electrophoresed in formaldehyde-denatured agarose gels. BGI (Huada Genomics Institute Co. Ltd., China) processed the Solexa sequencing of small RNAs.

Analysis of small RNA sequences

Small RNA-seq data were analyzed by using a custom-built pipeline that included 3 steps: adaptor/tag removal, genomic alignment, and miRBase comparison. The transcribed miRNAs and their expression levels were identified and measured. First, we removed extraneous sequences (the barcode tag and the Illumina adaptor) of each read from the 5' and 3' ends, respectively. Next, Bowtie was used to align reads to the hg19 reference genome assembly and RefSeq. The alignment location was compared with known miRNA genes in miRBase. The miRBase-defined miRNA was counted according to the overlapping reads (>50%). miRNA expression was measured by edgeR to compare control and PAHs-treated samples.

Differential expression analysis

The differential expression of miRNAs was processed in 2 steps. First, the expression of miRNAs in the 2 samples was normalized by TMM method from edgeR. Then, the fold change and P value were calculated from the normalized expression values.
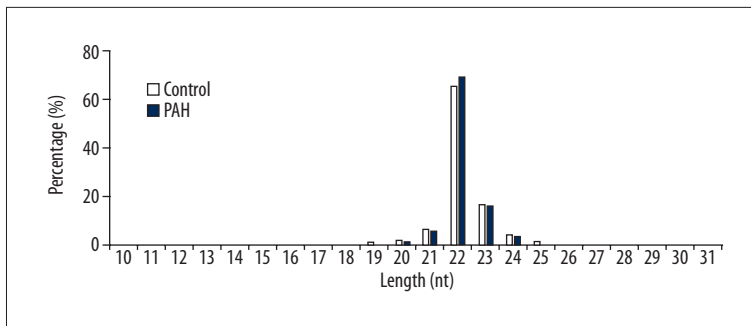
Figure 1. Distribution of read length. In the control sample, Raw reads were detected after Solexa sequencing. After we removed contaminant reads and low-quality reads, the remaining reads were uploaded and subjected to a length distribution analysis. Note that the 22 nt is the most frequent read length in both control and PT samples, followed by 23 nt, which made up 69.38% and 16.55% of total reads, respectively.

miRNA target prediction

The M3RNA database was used to predict miRNA-miRNA interactions. A new web-based algorithm *http://m3rna.cnb.csic. es/* was used for further analysis. This algorithm predicted miRNA targets based on information combined from 4 databases: Tarbase, miRTarBase, miRWalk, and miRecords. Nine different algorithms were used in these databases, including DIANA-microT, Microcosm, Microrna.org, TargetScan, Mirtarget, PITA, miRWalk-predictive, and TargetSpy.

GO and KEGG analysis

Tools from the DAVID database were used to perform the GO functional analysis of predicted miRNA target genes. The significantly enriched (P value <0.05) GO terms and KEGG terms were identified by comparison to the genome background. The default parameters were used.

qRT-PCR analysis

A First-Strand cDNA Synthesis Kit was used to synthesize cDNA from 1 μg of total RNA according to the manufacturer's instructions. TransStart Top Green qPCR SuperMix (Transgen Biotech) and an iQTM5 Multicolor Real-Time PCR Detection System (BIO-RAD) were used to perform qRT-PCR. The process of qRT-PCR was as follows: 95°C for 3 min, followed by 40 cycles at 95°C for 10 s, 60°C for 20 s, 72°C for 30 s, and 80°C for 10 s, and then 72°C for 5 min, and finally increases of 0.5°C every 10 s from 55°C to 95°C. The relative fold-changes of gene expression were calculated by the $2^{-\Delta\Delta Ct}$ method.

Results

Cell viability

Different concentrations (0, 100, 200, 300, 400, and 500 μg/ml) of PAHs solutions isolated from PM2.5 particles were added to HUVEC culture medium for 24 h before MTT assays. MTT assays were performed by measuring the absorbance value (OD value) at 492–630 nm on a microplate reader. Analysis of

MTT assay results showed that the IC50 of PAHs in HUVECs was 112.0925 μg/ml.

Global sequence analysis of small RNAs

To understand the miRNA regulation in ECs after PAH treatments, an sRNA library was constructed by extracting total RNA from ECs with and without PAHs treatment. The array results of each sample were confirmed for 3 times. In the control sample, a total of 13 000 000 raw reads were detected after Solexa sequencing. Contaminant reads and low-quality reads were removed. The remaining reads were uploaded and subjected to a length distribution analysis. The results showed that the most frequent read length was 22 nt followed by 23 nt, which made up 69.38% and 16.55% of total reads, respectively (Figure 1). Reads smaller than 18 nt and reads with poly(A) tails were then filtered to obtain a total of 12 733 284 clean reads (Table 1). Subsequently, clean reads were aligned against the human genome. In the PAHs-treated (PT) sample, a total of 13 000 000 raw reads were detected. The most frequent read lengths were 22 nt (65.59%) and 23 nt (16.86%) (Figure 1). In total, 12 572 254 clean reads were obtained after filtering (Table 1).

Statistical analysis was performed to compare the total and unique small RNAs in control and PT samples (Table 2). There were 25 305 538 total small RNAs, and the proportion of shared small RNAs between control and PT samples was 98.17% (24 841 988). The control-specific and PT-specific small RNAs were 0.74% (186 002) and 1.10% of the total, respectively. A total of 445 937 unique small RNAs were identified. Among them, 51 025 were found in both the control and PT samples. The numbers of unique sRNAs specific to the control and PT samples were 160 522 and 234 390, respectively.

Next, sRNAs were classified into different categories based on annotation and biogenesis by using alignments against the human genome on Rfam, GenBank, repeat-associated RNA, and miRbase (Table 3). The proportion of unannotated sRNAs in the control sample was 57.43%. In the PT sample, the representation of categories was as follows (Table.3). In the PT

Table 1. Filtering of raw reads from control and PAHs treated (PT) samples.

Type	Control		PT	
	Count	Percent (%)	Count	Percent (%)
Total reads	13000000		13000000	
High quality	12908352	100%	12901526	100%
3'adapter null	1236	0.01%	1385	0.01%
Insert null	6860	0.05%	9319	0.07%
5'adapter contaminants	149049	1.15%	242682	1.88%
Smaller than 18nt	17546	0.14%	75057	0.58%
polyA	377	0.00%	829	0.01%
Clean reads	12733284	98.64%	12572254	97.45%

PAHs – polycyclic aromatic hydrocarbons; PT – PAHs-treated.

Table 2. Comparing of total and unique small RNAs in control and PT samples.

Class	Control		PT	
	Unique sRNAS	Percent (%)	Total sRNAS	Percent (%)
Total sRNAs	445937		25305538	
Control & PAHs	51025	0.1144	24841988	0.9817
Control specific	160522	0.36	186002	0.0074
PAHs specific	234390	0.5256	277548	0.011

PAHs – polycyclic aromatic hydrocarbons; PT –PAHs-treated.

Table 3. The proportions of different kinds of sRNAs.

Category	Control				PT			
	Unique sRNAs	(%)	Total sRNAs	(%)	Unique sRNAs	(%)	Total sRNAs	(%)
Total	211547		12733284		285415		12572254	
Exon antisense	1259	0.006	1745	0.0001	1991	0.007	3196	0.0003
Exon sense	23288	0.1101	38678	0.003	41531	0.1455	53052	0.0042
Intron antisense	3580	0.0169	4292	0.0003	5862	0.0205	6993	0.0006
Intron sense	11905	0.0563	17179	0.0013	31073	0.1089	36856	0.0029
miRNA	4910	0.0232	10568984	0.83	5243	0.0184	10215373	0.8125
rRNA	18664	0.0882	108849	0.0085	24977	0.0875	163420	0.013
repeat	12196	0.0577	44802	0.0035	25882	0.0907	63001	0.005
scRNA	941	0.0044	9889	0.0008	1807	0.0063	21677	0.0017
snRNA	2307	0.0109	61367	0.0048	3840	0.0135	67194	0.0053
snoRNA	1306	0.0062	21822	0.0017	2193	0.0077	41578	0.0033
srpRNA	44	0.0002	62	0	54	0.0002	84	0
tRNA	9661	0.0457	149086	0.0117	11932	0.0418	160619	0.0128
Unann	121486	0.5743	1706529	0.134	129030	0.4521	1739211	0.1383

PT – PAHs-treated.

Table 4. KEGG analysis of putative miRNA targets predicted by the miRanda algorithm.

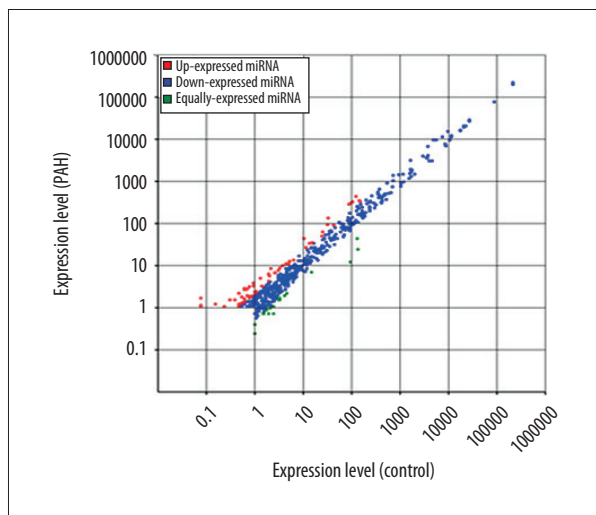|	Pathway	Target genes with pathway annotation (24054)		All genes of the species with pathway annotation (27635)		P value	Q value	Pathway ID
Known miRNA	Olfactory transduction	535	(2.22%)	564	(2.04%)	3.9E-10	1.2E-07	ko04740
	Axon guidance	481	(2%)	522	(1.89%)	0.00013	0.01437	ko04360
	Insulin signaling pathway	383	(1.59%)	413	(1.49%)	0.00014	0.01437	ko04910
	Small cell lung cancer	247	(1.03%)	263	(0.95%)	0.00021	0.0161	ko05222
Novel miRNA	Olfactory transduction	535	(2.22%)	564	(2.04%)	3.9E-10	1.2E-07	ko04740
	Axon guidance	481	(2%)	522	(1.89%)	0.00013	0.01437	ko04360
	Insulin signaling pathway	383	(1.59%)	413	(1.49%)	0.00014	0.01437	ko04910
	Small cell lung cancer	247	(1.03%)	263	(0.95%)	0.00021	0.0161	ko05222

Figure 2. Scatter plot of miRNAs expression between control and PT samples. Note that red and green plots are upregulated and downregulated, respectively. There were 77 known miRNAs that were significantly differentially expressed; 24 known miRNAs had high abundance (>10) in the samples; and a total of 22 novel miRNAs with significant differential expression were identified, 11 of which were downregulated.

sample, unannotated sRNAs made up 45.21% of the unique sRNAs. In general, these results suggest that miRNAs in the sRNA library were abundant in both samples.

Identification of known and novel miRNAs

After miRBase alignment using miRAlign, the known miRNAs in ECs were identified from candidate miRNA sequences. In total, 214 and 223 known miRNAs were identified in the control

and PT samples, respectively. Both samples had approximately 800 miRNA precursors. The 2 samples shared 502 known miRNAs or miRNA precursors (Table 4). The novel miRNAs were predicted from unannotated sRNAs by Mireap software, which examines the secondary structure, minimum free energy, and the Dicer cleavage site of sRNAs matched to the genome. A total of 59 novel miRNAs were predicted in the control sample, 78 were predicted in the PT sample, and 36 novel miRNAs were found in both samples.

Differential expression of known and novel miRNAs

The differentially expressed miRNAs were determined by comparing the miRNA expression between the control and PT samples (Table 4, Figure 2). There were 77 known miRNAs that were significantly differentially expressed, 24 known miRNAs had high abundance (>10) in the samples, and 6 level groups of miRNAs were clustered according to their fold change of expression in PT sample (Figure 3A). The miRNA has-miR-532-5p was found to be the most strongly downregulated (8-fold) known miRNA, while has-miR-579-5p was the most strongly upregulated (4-fold). A total of 22 novel miRNAs with significant differential expression were identified, 11 of which were downregulated. Novel-mir-53 and novel-mir-6 were downregulated in the PT sample but had high abundance in the control sample (>10).

Putative target genes

Putative target genes of differentially expressed miRNAs were predicted by the miRanda algorithm. There were 31 011 putative transcription products found for the 77 known miRNAs that were differentially expressed in the control and PT samples. According to GO functional analysis, these target genes
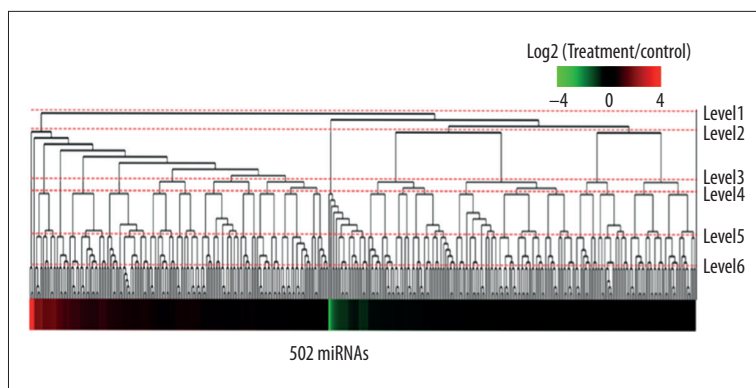
Figure 3A. Six level clusters of miRNA expression. Heat map for scaled miRNA expression ratio of PT divided by control that shows upregulated miRNAs (red region) and downregulated miRNAs (green region). miRNAs were ranked by log fold change in each regulated group.

Table 5. miRNAs with significantly change in PT sample. Down-regulated, log2 PT/control <-2; up-regulated, log2 PT/control >2.

miR-name	Control	PT	log2 PT/control	p-value
hsa-miR-3613-5p	0.08	1.67	4.41	5E–06
hsa-miR-376c-5p	0.08	1.11	3.83	0.000474
hsa-miR-376b-5p	0.08	1.03	3.72	0.000898
hsa-miR-652-5p	0.16	1.19	2.92	0.001198
hsa-miR-3648	0.31	1.51	2.27	0.00139
hsa-miR-7641	0.31	1.51	2.27	0.00139
hsa-miR-98-3p	0.47	2.15	2.19	0.000169
hsa-miR-4485	0.63	2.86	2.19	1.27E–05
hsa-miR-585-3p	0.63	2.86	2.19	1.27E–05
hsa-miR-31-3p	0.24	1.03	2.13	0.01183
hsa-miR-299-5p	10.37	43.43	2.07	4.99E–62
hsa-miR-3917	0.63	2.62	2.06	5.8E–05
hsa-miR-155-3p	0.94	3.82	2.02	1.55E–06
hsa-miR-99b-3p	135.86	23.86	−2.51	4.5E–240
hsa-miR-532-5p	94.24	11.85	−2.99	1E–201

are classified in diverse functional categories, including immune system process, multicellular organismal process, reproductive process, response to stimulus, rhythmic process, cell junction, and cell death. Furthermore, GO enrichment analysis revealed that these target genes are widely spread in diverse biological processes. Next, all putative target genes corresponding to the known miRNAs were subjected to KEGG analysis. The results showed that genes related to olfactory transduction, axon guidance, insulin signaling, and small cell lung cancer were significantly enriched compared with genes in the whole human genome (Table 4).

For the 22 novel miRNAs, 29 399 transcription products were obtained as putative targets. After GO analysis, it was shown that these genes were widely spread in diverse biological processes without significant enrichment. Similar to the known miRNA targets, KEGG analysis showed that the significantly enriched genes were related to olfactory transduction, axon guidance, insulin signaling, and small cell lung cancer (Table 4). In general, the PT-regulated miRNAs were targeted to almost the whole genome, and the specific function of these miRNAs remains elusive.

Mature miRNAs have a highly conserved seed region at position 2~8, while the target sequences might be different in this region. This phenomenon is called miRNA base editing and can be detected by aligning unannotated sRNA tags with mature miRNAs from miRBase. In this study, miRNAs allowing 1 mismatch with their putative targets in certain positions were identified. In the control sample, 73 miRNAs had less than 5% base editing, while 27 miRNAs had more than 95% base editing. In the PT sample, 149 miRNAs had less than 5% base editing and 49 had more than 95% base editing.
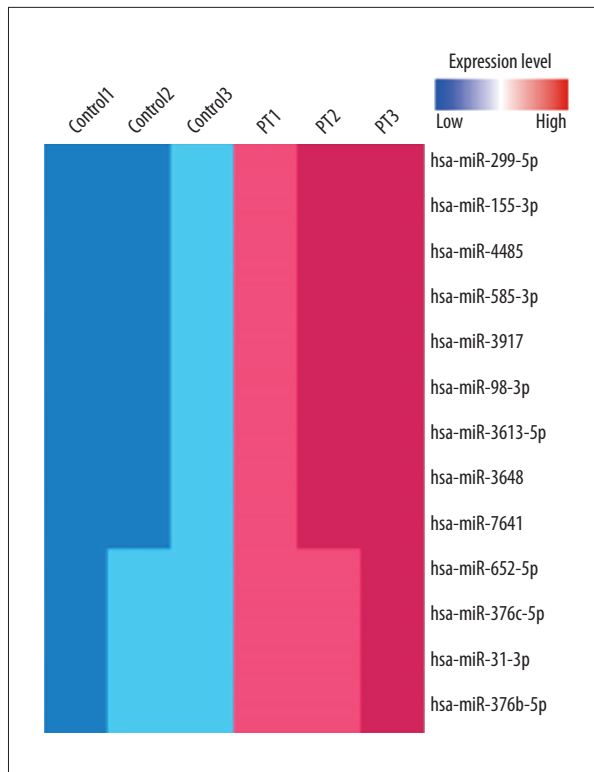
Figure 3B. The 13 upregulated known miRNAs. The miRNAs expression of 3 replicates of control and 3 replicates of PT show less variants among replicates. We used 4-fold change as a strict cutoff.

Function of significantly upregulated and downregulated known miRNAs in cardiovascular development and disease

According to the miRanda algorithm, the regulated miRNAs in the PT sample could target the global genome. To better understand the function of regulated miRNAs in the PT sample, we used a new predictive combined database that can more precisely predict the miRNA-miRNA interactions.

Two significantly downregulated (>4-fold) known miRNAs – has-miR-99b-3p and has-miR-532-5p – were identified in the PT sample and corresponded to 5323 putative target genes. These putative target genes were enriched in some general biological processes, such as the regulation of transcription, according to GO and KEGG analyses (Table 5).

In the PT sample, 13 significantly upregulated (>4-fold) known miRNAs were identified: hsa-miR-155-3p, hsa-miR-376c-5p, hsa-miR-376b-5p, hsa-miR-652-5p, hsa-miR-3648, hsa-miR-7641, hsa-miR-98-3p, hsa-miR-4485, hsa-miR-585-3p, hsa-miR-3613-5p, hsa-miR-299-5p, hsa-miR-3917, and hsa-miR-31-3p (Figure 3B).

To precisely understand the function of the other miRNAs, an improved algorithm was applied to predict their targets. From multiple miRNA-miRNA interaction databases, 5791 genes were identified as putative targets with diverse biological functions (Table 6). According to GO analysis, enrichment was observed in genes involved in general biological processes such as regulation of transcription, protein location, and protein transport. However, we also observed significant enrichment of genes involved in some special processes, such as neuron

Table 6. GO and KEGG analysis of putative miRNA targets predicted by the miRNA database.

Term	Count	%	P value
Schizophrenia; bipolar disorder	14	0.243224	0.002952
Hypertension	72	1.250869	0.03269
GO: 0048666~neuron development	140	2.432245	3.48E-05
GO: 0048598~embryonic morphogenesis	128	2.223767	4.62E-05
GO: 0016568~chromatin modification	116	2.015288	4.99E-05
GO: 0001568~blood vessel development	105	1.824183	6.55E-05
GO: 0001944~vasculature development	107	1.85893	7.19E-05
Schizophrenia; bipolar disorder	14	0.243224	0.002952
Hypertension	72	1.250869	0.03269
hsa04310: Wnt signaling pathway	75	1.302988	4.1E-07
hsa04930: Type II diabetes mellitus	28	0.486449	7.11E-05
hsa05200: Pathways in cancer	130	2.258513	9.45E-05
hsa04012: ErbB signaling pathway	43	0.747047	0.000204

development (P value, 3.48E-05), embryonic morphogenesis (P value, 4.62E-05), chromatin modification (P value, 4.99E-05), blood vessel development (P value, 6.55E-05), and vasculature development (P value, 7.11E-05). In addition, these genes were subjected to KEGG pathway analysis. The results showed that genes in the Wnt signaling pathway (P value, 4.10E-07), type II diabetes mellitus (P value, 7.11E-05), cancer pathways (P value, 9.45E-05), and the ErbB signaling pathway (P value, 2.04E-04) were significantly enriched.

qRT-PCR analysis of predicted target genes

To understand the expression pattern of putative target genes related to cardiovascular development and disease, a qRT-PCR analysis was performed. Downregulated expression was detected for the 8 common genes (186, 1906, 1909, 2022, 2702, 3553, 3953, 51752) involved in blood vessel development, vasculature development and hypertension, which were putative targets of upregulated miRNAs in PAHs-treated cells (Figure 4).

Figure 4. RT-PCR analysis of putative targets of miRNA upregulated by PAH treatment. Downregulated expression was detected for the 8 common genes (186, 1906, 1909, 2022, 2702, 3553, 3953, 51752) involved in blood vessel development, vasculature development, and hypertension, which were putative targets of upregulated miRNAs in PAHs-treated cells.

Discussion

In this study, we identified 2 downregulated and 14 upregulated known miRNAs with significant changes in expression. Among these genes, miRNA-155 has a well-known role in vascular development and disease. By integrating miRNA and putative target gene prediction, 5791 genes were identified as putative targets. These enriched genes were involved in biological processes related to vascular development such as blood vessel development, vasculature development, hypertension, Wnt signaling, and ErbB signaling. These results reveal a possible mechanism of PAHs-induced cardiovascular disease through miRNA expression.

miR-155 has confirmed targets, including SOCS1, TAB2, PU.1, AT1R, ETS-1, BCL6, CCL2, HMGB1, MMP1, and MMP3. These genes are involved in diverse biological processes related to cardiovascular development and disease, such as pro-inflammatory and anti-inflammatory signaling, HUVEC activation and migration, angiogenesis, arteriogenesis, atherosclerosis, foam cell formation, and matrix degradation. It has been shown that the interleukin-1 signaling pathway is regulated by miRNA-155 in activated human monocyte-derived dendritic cells [16]. miRNA-155 is also an adverse mediator of cardiac injury and dysfunction during acute viral myocarditis [17]. Angiotensin II-induced endothelial inflammation and migration are regulated by microRNA-155 [18]. During adaptive neovascularization, miRNA-155 plays an important role in cell-specific antiangiogenesis [19]. Atherosclerosis is promoted by miRNA-155 through the repression of Bcl6 [20]. Foam cell formation is also accelerated by elevated miRNA-155 and subsequent repression of HBP1 [21]. In summary, miRNA-155
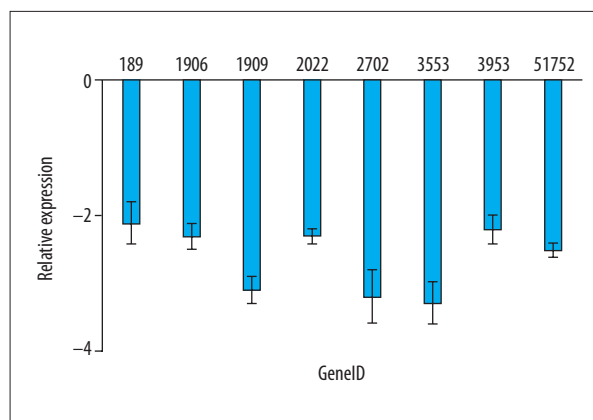
up-regulation after PAHs treatment plays a major role in cardiovascular development and disease. According to GO analysis, enrichment was observed in genes involved in general biological processes such as regulation of transcription, protein location, and protein transport. In addition, these genes were subjected to KEGG pathway analysis. The results showed that genes in the Wnt signaling pathway (P value, 4.10E-07), type II diabetes mellitus (P value, 7.11E-05), cancer pathways (P value, 9.45E-05), and the ErbB signaling pathway (P value, 2.04E-04) were significantly enriched.

According to the GO and KEGG pathway analyses, the upregulated miRNAs were indicated to play vital functions in cardiovascular development and disease. Genes involved in blood vessel development, vasculature development, and hypertension, which were putative targets of PT-induced miRNAs, were obviously related to cardiovascular development and disease. There were 105, 107, and 72 putative target genes of upregulated miRNAs in PAHs-treated cells related to blood vessel development, vasculature development, and hypertension, respectively. ATGR2 (186) encodes an angiotensin II receptor type 2 protein that plays an important role in mediating cell death during development and pathophysiology [22]. Endothelin 1 (EDN1) (1906) is a preproprotein that produces a secreted peptide belonging to the endothelin/sarafotoxin family. Recently, EDN1 was identified as a marker for pulmonary arterial hypertension in HIV infection [23]. Endothelin receptor type A (EDNRA) (1909) is a receptor for EDN1. Endoglin (ENG) (2022) is a major glycoprotein in the vascular endothelium. Endoplasmic reticulum aminopeptidase 1 (EEAP1) (51752) is involved in blood pressure regulation by inactivation of angiotensin II [24].

Recent studies show that chromatin modification is one of the major mechanisms controlling cardiac gene function. For instance, pharmacological inhibition of members of the histone deacetylase (HDAC) family, which are components of chromatin modification complexes, can prevent heart failure through regulating expression of related genes, such as the histone methyltransferase (HMT) enhancer of zeste homolog 2 (Ezh2), which is associated with pathological cardiac hypertrophy [25]. We identified 116 putative target genes of upregulated miRNAs in the PT sample that were related to chromatin modification.

The Wnt signaling pathway plays diverse roles in crucial aspects of cardiovascular development and disease processes, including cardiac morphogenesis, differentiation of cardiac progenitor cells, and self-renewal [26–28]. Evidence demonstrates that cardiovascular defects lead to loss of Wnt signaling [29]. There were 75 putative target genes of upregulated miRNAs in PT samples that were related to the Wnt signaling pathway.

ErbB signaling, which plays essential roles in cancer, was also implicated in CVDs [30]. Cancer therapies targeting ErbB signaling revealed its role in the maintenance of cardiac function [31]. Neuregulin 1 (NRG1) in the ErbB signaling pathway can regulate diverse processes in cardiovascular biology, such as blood pressure and angiogenesis. Forty-three putative target genes of upregulated miRNAs in the PT samples were related to the ErbB signaling pathway.

Conclusions

In general, this study suggests that PAHs taken by PM2.5 can downregulate CVDs-related gene expression through upregulating miRNA, which may be new target for therapy in the future.

Conflict of interest

None.

References:

1. Dominici F, Peng RD, Bell ML et al: Fine particulate air pollution and hospital admission for cardiovascular and respiratory diseases. JAMA, 2006; 295(10): 1127–34

2. Stafoggia M, Cesaroni G, Peters A et al: Long-term exposure to ambient air pollution and incidence of cerebrovascular events: Results from 11 European cohorts within the ESCAPE project. Environ Health Perspect, 2014; 122(9): 919–25

3. Liu C, Fonken LK, Wang A et al: Central IKKbeta inhibition prevents air pollution mediated peripheral inflammation and exaggeration of type II diabetes. Part Fibre Toxicol, 2014; 11: 53

4. Brook RD, Franklin B, Cascio W et al: Air pollution and cardiovascular disease: a statement for healthcare professionals from the Expert Panel on Population and Prevention Science of the American Heart Association. Circulation, 2004; 109(21): 2655–71

5. Brook RD, Rajagopalan S, Pope CA 3rd et al: Particulate matter air pollution and cardiovascular disease: An update to the scientific statement from the American Heart Association. Circulation, 2010; 121(21): 2331–78

6. Sun Q, Hong X, Wold LE: Cardiovascular effects of ambient particulate air pollution exposure. Circulation, 2010; 121(25): 2755–65

7. Jia X, Guo X, Li H et al: Characteristics and popular topics of latest researches into the effects of air particulate matter on cardiovascular system by bibliometric analysis. Inhal Toxicol, 2013; 25(4): 211–18

8. Kang YJ, Li Y, Zhou Z et al: Elevation of serum endothelins and cardiotoxicity induced by particulate matter (PM2.5) in rats with acute myocardial infarction. Cardiovasc Toxicol, 2002; 2(4): 253–61

9. Ito T, Suzuki T, Tamura K et al: Examination of mRNA expression in rat hearts and lungs for analysis of effects of exposure to concentrated ambient particles on cardiovascular function. Toxicology, 2008; 243(3): 271–83

10. Miyata R, Hiraiwa K, Cheng JC et al: Statins attenuate the development of atherosclerosis and endothelial dysfunction induced by exposure to urban particulate matter (PM10). Toxicol Appl Pharmacol, 2013; 272(1): 1–11

11. Han Wei, Dan Wei, Shuo Y et al: Oxidative stress induced by urban fine particles in cultured EA.hy926 cells. Hum Exp Toxicol, 2011; 30(7): 579–90

12. Welten SM, Goossens EA, Quax PH1, Nossent AY et al: The multifactorial nature of microRNAs in vascular remodelling. Cardiovasc Res, 2016; 110(1): 6–22

13. Zhao D, Wang Y, Luo D et al: PMirP: A pre-microRNA prediction method based on structure-sequence hybrid features. Artif Intell Med, 2010; 49(2): 127–32

14. Faccini J, Ruidavets JB, Cordelier P et al: Circulating miR-155, miR-145 and let-7c as diagnostic biomarkers of the coronary artery disease. Sci Rep, 2017; 7: 42916

15. Jansen F, Stumpf T, Proebsting S et al: Intercellular transfer of miR-126-3p by endothelial microparticles reduces vascular smooth muscle cell proliferation and limits neointima formation by inhibiting LRP6. J Mol Cell Cardiol, 2017; 104: 43–52

16. Ceppi M, Pereira PM, Dunand-Sauthier I et al: MicroRNA-155 modulates the interleukin-1 signaling pathway in activated human monocyte-derived dendritic cells. Proc Natl Acad Sci USA, 2009; 106(8): 2735–40

17. Corsten MF, Papageorgiou A, Verhesen W et al: MicroRNA profiling identifies microRNA-155 as an adverse mediator of cardiac injury and dysfunction during acute viral myocarditis. Circ Res, 2012; 111(4): 415–25

18. Zhu N, Zhang D, Chen S et al: Endothelial enriched microRNAs regulate angiotensin II-induced endothelial inflammation and migration. Atherosclerosis, 2011; 215(2): 286–93

19. Pankratz F, Bemtgen X, Zeiser R et al: MicroRNA-155 exerts cell-specific antiangiogenic but proarteriogenic effects during adaptive neovascularization. Circulation, 2015; 131(18): 1575–89

20. Nazari-Jahantigh M, Wei Y, Noels H et al: MicroRNA-155 promotes atherosclerosis by repressing Bcl6 in macrophages. J Clin Invest, 2012; 122(11): 4190–202

21. Tian FJ, An LN, Wang GK et al: Elevated microRNA-155 promotes foam cell formation by targeting HBP1 in atherogenesis. Cardiovasc Res, 2014; 103(1): 100–10

22. Zhao Y, Lützen U, Fritsch J et al: Activation of intracellular angiotensin AT(2) receptors induces rapid cell death in human uterine leiomyosarcoma cells. Clin Sci (Lond), 2015; 128(9): 567–78

23. Parikh RV, Ma Y, Scherzer R et al: Endothelin-1 predicts hemodynamically assessed pulmonary arterial hypertension in HIV infection. PLoS One, 2016; 11(1): e0146355

24. Stamogiannos A, Koumantou D, Papakyriakou A, Stratikos E: Effects of polymorphic variation on the mechanism of Endoplasmic Reticulum Aminopeptidase 1. Mol Immunol, 2015; 67(2 Pt B): 426–35

25. Mathiyalagan P, Keating ST, Du XJ, El-Osta A: Chromatin modifications remodel cardiac gene expression. Cardiovasc Res, 2014; 103(1): 7–16

26. Nakamura K, Sano S, Fuster JJ et al: Secreted frizzled-related protein 5 diminishes cardiac inflammation and protects the heart from ischemia/reperfusion injury. J Biol Chem, 2016; 291(6): 2566–75

27. Rai M, Walthall JM, Hu J, Hatzopoulos AK: Continuous antagonism by Dkk1 counter activates canonical Wnt signaling and promotes cardiomyocyte differentiation of embryonic stem cells. Stem Cells Dev, 2012; 21(1): 54–66

28. Cohen ED, Tian Y, Morrisey EE: Wnt signaling: An essential regulator of cardiovascular differentiation, morphogenesis and progenitor self-renewal. Development, 2008; 135(5): 789–98

29. Tian Y, Yuan L, Goss AM et al: Characterization and *in vivo* pharmacological rescue of a Wnt2-Gata6 pathway required for cardiac inflow tract development. Dev Cell, 2010; 18(2): 275–87

30. Lurje G, Lenz HJ: EGFR signaling and drug discovery. Oncology, 2009; 77(6): 400–10

31. Odiete O, Hill MF, Sawyer DB: Neuregulin in cardiovascular development and disease. Circ Res, 2012; 111(10): 1376–85